Bioorganic & Medicinal Chemistry 17 (2009) 6166–6172

Contents lists available at ScienceDirect

Bioorganic & Medicinal Chemistry

journal homepage: www.elsevier.com/locate/bmc

Inhibitory effect of β-diketones and their metal complexes on TNF-α induced expression of ICAM-1 on human endothelial cells

Francesco Caruso [a,*], Claudio Pettinari [b], Fabio Marchetti [b], Miriam Rossi [c], Cristian Opazo [d], Sarvesh Kumar [e], Sakshi Balwani [e], Balaram Ghosh [e,*]

[a] Istituto di Chimica Biomolecolare, Consiglio Nazionale delle Ricerche (CNR), c/o Università di Roma 'La Sapienza', Vecchio Istituto Chimico, Piazzale Aldo Moro 5, 00185 Rome, Italy
[b] Dipartimento Scienze Chimiche, Università di Camerino, Via S. Agostino 1, 62032 Camerino (MC), Italy
[c] Department of Chemistry, Vassar College, Poughkeepsie, NY 12604-0484, USA
[d] Academic Computing Services CIS, Vassar College, Poughkeepsie, NY 12604-0748, USA
[e] Molecular Immunogenetics Laboratory, Institute of Genomics and Integrative Biology, University of Delhi Campus (North), Mall Road, Delhi 110 007, India

ARTICLE INFO

Article history:
Received 15 April 2009
Revised 22 July 2009
Accepted 26 July 2009
Available online 30 July 2009

Keywords:
Inflammation
Cell adhesion molecules
Human endothelial cells
Anti-inflammatory
Metal-β-diketones
DFT

ABSTRACT

Recent reports show that the natural β-diketone curcumin displays important biological properties regarding the intercellular adhesion molecule-1 (ICAM-1), which plays a critical role in the immune responses and inflammation. In this study the ICAM-1 inhibitory activity of β-diketone compounds, which are curcumin models lacking aromatic peripheral hydroxyl and methoxy groups, along with some metal derivatives is investigated. β-Diketones are systematically more active than metal complexes and the best obtained inhibition is 75% for both groups. The best inhibitors are 4-benzoyl-3-methyl-1-phenyl-pyrazol-5-one (HQ^{Ph}) among the ligands, and sodium benzoylacetonato among metal derivatives. These results appear in line with the reported antitumor activity of related species. Since 4-acyl-5-pyrazolones posses four tautomeric forms, those corresponding to HQ^{Ph} were investigated using density functional theory. Docking of all HQ^{Ph} tautomers on ICAM-1 protein was performed suggesting one keto-enol form favored to act in biological environment.

1. Introduction

The adhesion of leukocytes to the endothelium is among the earliest and most important process during any kind of inflammatory response.[1] The trans-endothelial migration of the leukocytes requires the increased expression of cell adhesion molecules on the surface of endothelial cells that interact with their corresponding receptors on the surface of leukocytes.[2] These leukocyte cell surface proteins are commonly known as cell adhesion molecules. The major cell adhesion molecules involved in this process are intercellular cell adhesion molecule-1 (ICAM-1), vascular cell adhesion molecule-1 (VCAM-1) and E-selectin expressed on endothelium in response to various cytokines or bacterial lipopolysaccharide.[3] The increased expression of cell adhesion molecules alters the adhesive property of the vasculature leading to indiscriminate infiltration of the leukocytes across the blood vessels and hence inflammation.[4–6] A regulated expression of cell adhesion molecules is therefore essential for maintaining the body fluidity. Inhibition of cell adhesion molecules is a useful therapeutic approach to regulate inflammatory response.[7] Small molecules from natural and synthetic sources have been used successfully for down regulating the induced expression of cell adhesion molecules both in vitro and in vivo.[8–12] Several medicinal herbs have been shown to augment specific cellular and humoral immune responses.[13–16]

Curcumin, an important component of curry, is a natural antioxidant and antitumor polyphenol β-diketone isolated from *Curcuma longa*. Recently, it was shown that the expression of ICAM-1 was attenuated by curcumin at both mRNA and protein levels.[17] Also, pretreatment with curcumin blocked interleukin-1 β induced ICAM-1 expression in A549 cells.[18] In addition, the antitumor effect of gemcitabine (the best treatment available for pancreatic cancer) is potentiated by curcumin through suppression of proliferation, angiogenesis and inhibition of nuclear factor-κB-regulated gene products.[19] Moreover, reduction of matrixmetalloproteinase-2 activity and inhibition of carcinoma HEP2 cell invasion by curcumin, strongly indicates the potential of curcumin as an inhibitor of tumor cell invasion and metastasis.[20] Furthermore, intratracheal injection of bleomycin to rats induces acute lung

Abbreviations: ICAM-1, intercellular adhesion molecule-1; VCAM-1, vascular cell adhesion molecule-1; TNF-α, tumor necrosis factor-α; HUVEC, human umbilical vein endothelial cells.

* Corresponding authors. Tel.: +39 06 49913632; fax: +39 06 49913628 (F.C.); tel.: +91 11 2766 2580; fax: +91 11 2766 7471 (B.G.).
E-mail addresses: caruso@vassar.edu (F. Caruso), bghosh@igib.res.in (B. Ghosh).

0968-0896/$ - see front matter © 2009 Elsevier Ltd. All rights reserved.
doi:10.1016/j.bmc.2009.07.064

injury accompanied by increased lung levels of intercellular ICAM-1 seven days after bleomycin administration. However, curcumin treatment significantly inhibited bleomycin-induced effects and restored the levels of antioxidant enzymes to normal values.[21]

Several years ago we initiated a systematic study using 4-acyl-5-pyrazolones (Scheme 1) as ligands for several metal cations and some of their related complexes showed marked antitumor activity.[22,23] 4-Acyl-5-pyrazolones are a class of asymmetric β-diketones that differ from curcumin by lacking aromatic hydroxyl and methoxy substituents. Since their biological activity should be due only to the diketo moiety, they provide indirect information about the mechanism of action of curcumin. In this study, we investigate the inhibition of cell surface expression of ICAM-1 by several diketones along with their metal complexes, and attempt to clarify the underlying chemical mechanism behind the inhibition. The study includes an ICAM-1 docking for the best found inhibitor, clarifying the related tautomer preference.

2. Results and discussion

The tested compounds were found to be non-toxic up to their maximum tolerable concentrations as shown in Table 1. We have found that more than 95% cells were viable at these concentrations (Table 1). At the same time, DMSO (used as a solvent) was also not causing any cytotoxic effect to endothelial cells. These data show that these compounds are safe for endothelial cells.

Tested compounds in this study are shown in Scheme 2 while Table 1 indicates that although the maximum level of inhibition is the same for ligands and metal complexes (75%), the concentration needed for such an endeavor is always higher for the latter. It appears that the ligands are more effective in the used model because of a straightforward interaction with the target. Therefore, the effect of the metal in their complexes seems to be to decrease ligand availability. On the contrary, antitumor studies of titanium β-diketonates show the Ti-β-diketone binding is strong and necessary for biological activity. In fact, titanium complexes were the most active metal derivatives in studies performed by Keppler.[24,25] We conclude that there is no potential benefit of ligand protection though metal coordination in the present model. The antitumor activity in Keppler's studies show benzoylacetonato to be the best ligand for Ti complexes. Interestingly, benzoylacetonato, used in compound **C-4**, gives the best inhibition in this study among metal derivatives (**C-1** to **C-6**). Consistently, HQ^{Ph} is the the most active among all tested ligands (**L-1** to **L-6**), and forms a Ti complex with antitumor activity[22] of the same order (T/C around 300%) than the best one in Keppler studies.[25] Therefore, we selected HQ^{Ph} and proceeded to test its activity at lower concentration. First we analyzed viability, Figure 1, and found that HQ^{Ph} is less cytotoxic than curcumin, as the maximum tolerable doses are 100 μg/ml = 271.4 μM/ml and 50 μM/ml,[26] respectively. The specific inhibitor activity of

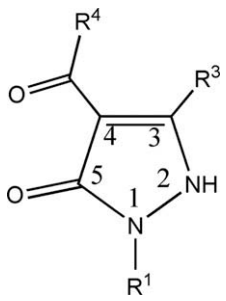

Scheme 1. 4-Acyl-5-pyrazolones, only compounds containing R^1 = Ph were used in the present study.

Table 1
ICAM-1 inhibitory activity of β-diketones and their metal complexes

Name of compound	Structure of compound	Concentration (μg/ml)	% Inhibition	% Viability
DMSO	Solvent	0.25%	—	97.1
C-1	$Ca(Q^{nPe})_2(EtOH)_2$	120	40	98.3
C-2	$Zn(Q^{nPe})_2(H_2O)_2$	35	35	96.4
C-3	NaQ^{Ph}	80	25	95.8
C-4	Na(bzac)	70	75	97.1
C-5	Na(bzfc)	80	45	96.0
C-6	$Zn(Q^{tBu})_2(H_2O)_2$	80	15	98.7
L-1	HQ^{Fur}	60	55	96.2
L-2	HQ^{Ph}	60	75	95.8
L-3	$HQ^{t\text{-}But}$	60	60	96.1
L-4	HQ^{EtCp}	60	35	98.6
L-5	HQ^{nPe}	60	35	97.1
L-6	$HQ^{Ph,Ph,Me}$	60	20	97.9

HQ^{Ph} is shown in Figure 2 with IC_{50} of 36.3 μg/ml. However, HQ^{Ph} shows only 62% ICAM-1 inhibition at the highest dose of 271.4 μM/ml (IC_{50} = 98.5 μM/ml) whereas curcumin[26] shows up to 90% ICAM-1 inhibition at the highest dose of 50 μM/ml. These data suggest that curcumin is more active than HQ^{Ph} in inducing the cytokine-induced expression of I-CAM-1 on HUVEC.

4-Acyl-5-pyrazolones can display several tautomeric forms shown in Scheme 3. To estimate the potential active form acting on ICAM-1 we calculate the molecular structure of each tautomer in water for the most active ligand found in this study, HQ^{Ph}, using density functional theory (DFT) and compare with X-ray structures in the literature,[27,28] see Table 2. Structural agreement between X-ray[27] and DFT methods is excellent for the N–H diketo form I; torsion angles of keto-enol II will be discussed later. DFT calculations show both diketo forms displaying the two carbonyls with O···O separations longer than 3 Å due to electronic repulsion, Figures 3 and 6, whereas both keto-enol structures allow a closer approach of both oxygens due to the linking intramolecular H-bond, Figures 4 and 5. Diffraction studies show 4-acyl-5-pyrazolonato metal complexes have a tendency for co-planarity of the pyrazole ring and its attached Ph. The expected torsion angles (closely related to the dihedral angle between both rings) should be about 0°, but crystal packing[29] can increase this value. In this study the DFT structures are exempt of packing effects as the molecule is calculated in water solution. We conclude that the X-ray torsion angle of the keto-enol tautomer II (−30.8° and 24.7°) do not compare well with the calculated DFT value (−2.0°) because of packing effects in the crystal[27] and so the DFT structure resembles better, in this case, the situation in the biological environment.

Similar torsion angles, far from co-planarity, found in the X-ray[27] (20.6°) and DFT (23.0°) structures of N–H diketo form are explained by a different factor, namely, the steric hindrance between the H bound to N and an *ortho*-H atom in the Ph ring. On the contrary, the C–H tautomer displays the H (of C) away from the Ph and the DFT structure shows more co-planarity with a torsion angle of 6.2°. There is no preference among both keto-enol forms (II and III) as their energy difference is only 1.0 kcal/mol. This contrasts with metal derivative structures that show preference for M–O(pyrazolonato) bond shorter than M–O(acyl), consistent with tautomer form II. A dynamic H atom moving between both oxygens would explain the DFT result. The energy difference (Delta E = 4.5 kcal/mol) between both diketo forms (C–H and N–H) favors the latter tautomer, which is consistent with the fact that the N–H tautomer is the one found in the crystal.[27] The energy difference between calculated structures of tautomers found in the crystalline state (keto-enol II and diketo N–H I) favors the former (Delta E = 3.7 kcal/mol), suggesting keto-enol as potentially more prone to act in biological environment.

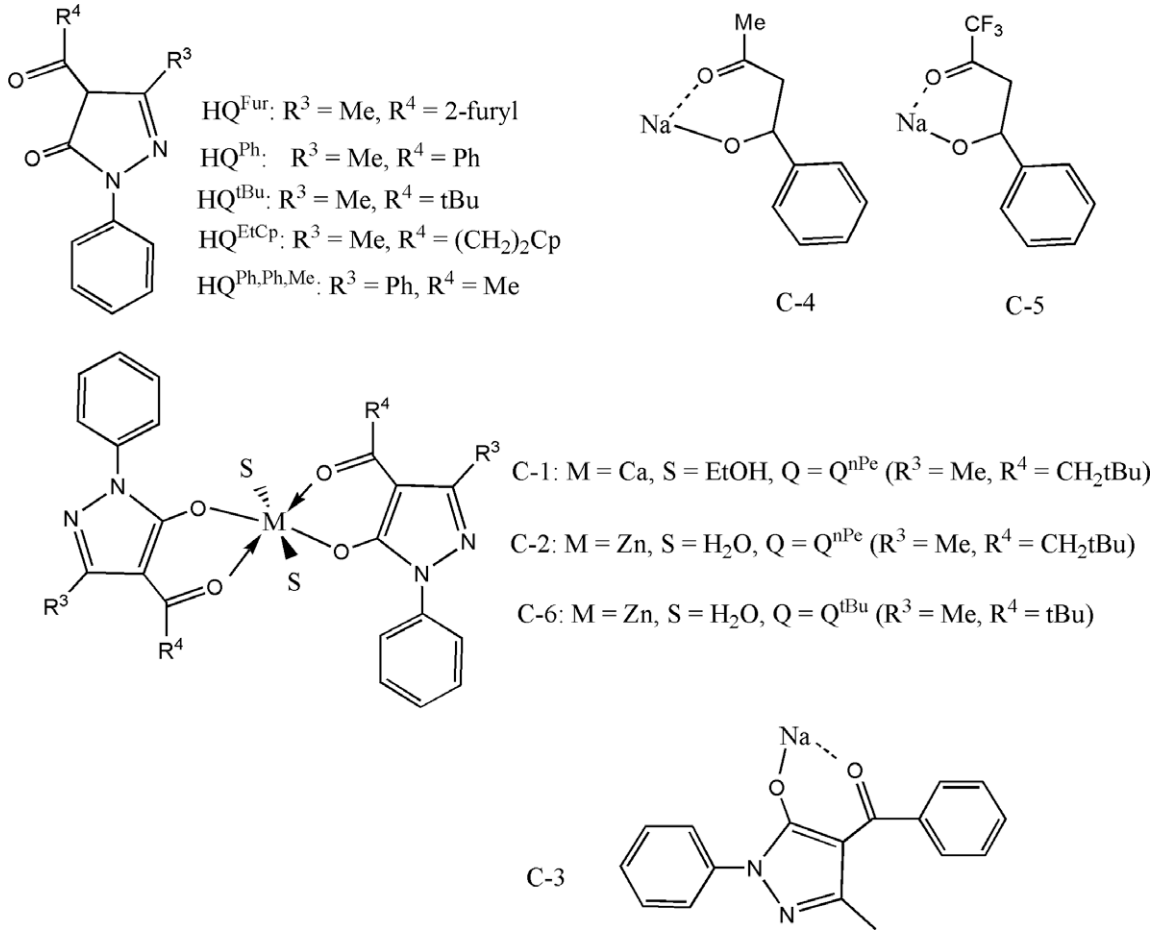

Scheme 2. Tested compounds.

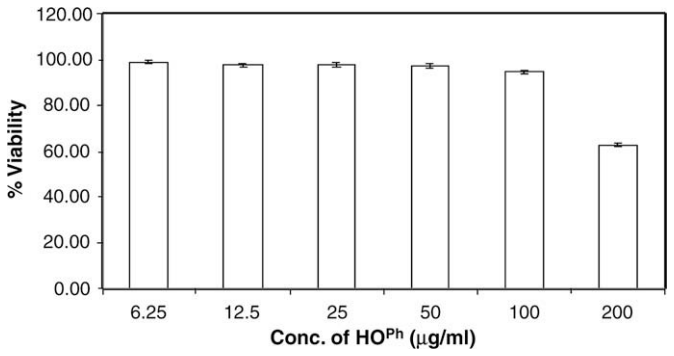

Figure 1. Cytotoxicity of HQ^{Ph} on human umbilical vein endothelial cells (HUVEC).

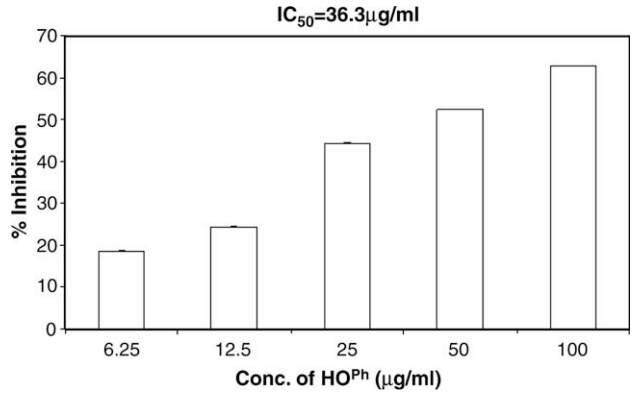

Figure 2. ICAM-1 inhibition of HQ^{Ph} on HUVEC.

Therefore, we performed a docking study on ICAM-1 to see its preference for HQ^{Ph} tautomers. Although there are no crystal structures including guests for this protein, a number of ICAM-1-binding isolates have been identified and analyzed in detail;[30] they all involve the L43 loop of ICAM-1 (aminoacids 42–49). Such loop has been recently successfully employed to design an inhibitor of *Plasmodium falciparium*, (+)-epigalloyl-catechin-gallate [(+)EGCG], after exploring *in silico* over 3 million commercial compounds.[31]

We proceeded extracting coordinates of ICAM-1 from the Protein Data Bank, PDB code 1IAM.[32] and performed the docking for the four tautomers plus (+)EGCG, operating with Discovery Studio 2.1. After CHARMm force-field H generation H coordinates in the active site were made consistent with the crystal structure. In a first simulation, the active site was kept fixed and the four tautomers and (+)EGCG in turn were allowed to fit. Ten poses were calculated for each guest and binding energy, which describes guest affinity for the active site pocket, was calculated for each molecule's pose. Later, ligand minimizations for the active site including, in turn, all docked molecules were performed. Energy affinity, Table 3, of the best fit molecules show that keto-enol (II) fits better than keto-enol (III), and, as mentioned earlier, this is consistent with all HQ^{Ph} metal derivatives showing structures having M–O(pyrazolonato) bond shorter than M–O(acyl). Interestingly, the affinity of the CH diketo (IV) tautomer is highest for all

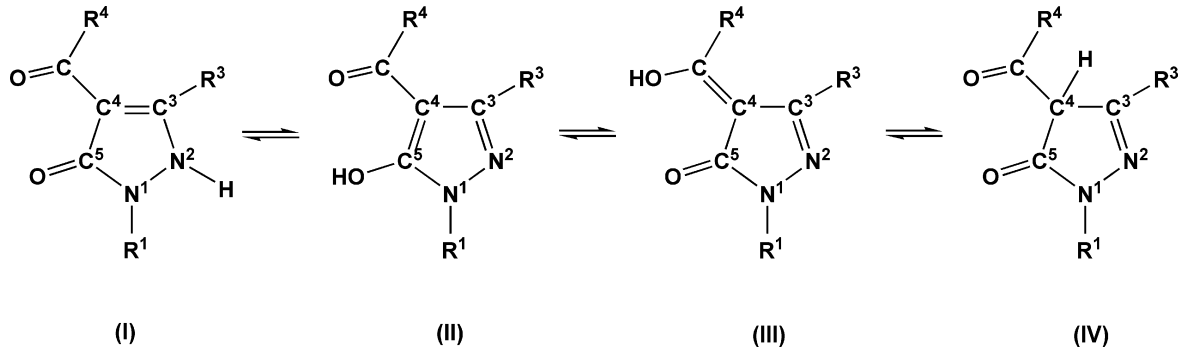

Scheme 3. Tautomer forms of 4-acyl-5-pyrazolones. I: N–H diketo, II: keto-enol(pyrazolone), III: keto-enol(acyl), IV: C–H diketo.

Table 2
Tautomer structures of HQ^{Ph}

Tautomer	Method	Torsion	*d*(C=O)	*d*(C–OH)	*d*(O···O)	Energy (–)
Diketo N–H (I)	X-ray DEBFAR[R1]	20.6	1,23, 1.24		3.08	
Diketo N–H (I)	DFT	23.0	1.239, 1.245		3.034	916.439002
Keto-enol (II) (*a*)	X-ray YUYDOL	−30.8	1.25	1.32	2.66	
Keto-enol (II) (*b*)	X-ray YUYDOL[R2]	24.7	1.24	1.32	2.62	
Keto-enol (II)	DFT	−2.0	1.277	1.323	2.495	916. 444969
Keto-enol (III)	DFT	−8.4	1.266	1.431	2.523	916.446720
Diketo C–H (IV)	DFT	6.2	1.230, 1.232		3.257	916.431832

Notes: R1 (DEBFAR) and R2 (YUYDOL) are refcodes in the crystal structure CSD database. The keto-enol form (YUYDOL) crystallizes with 2 independent molecules in the unit cell (*a* and *b*); their geometrical values are displayed in rows 4th and 5th. Energy unit: hartree; distances: Å.

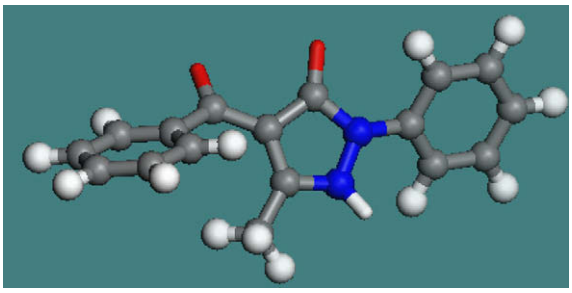

Figure 3. DFT calculated diketo N–H form I.

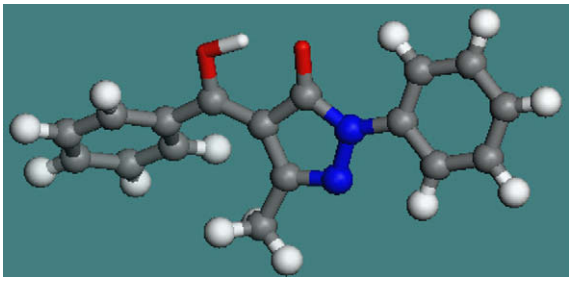

Figure 5. DFT calculated keto-enol form III, showing intramolecular hydrogen bond.

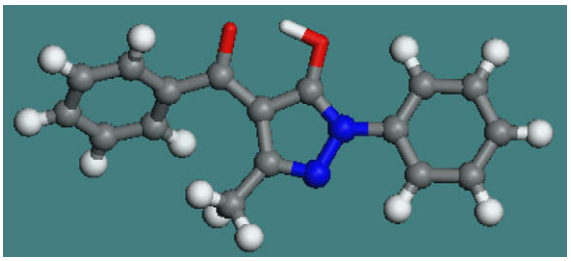

Figure 4. DFT calculated keto-enol form II, showing intramolecular hydrogen bond.

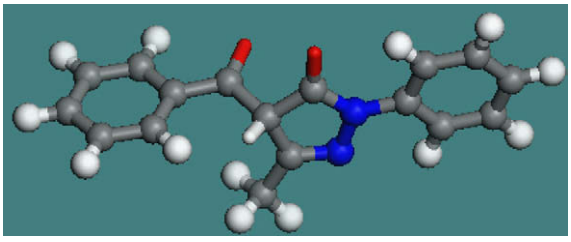

Figure 6. DFT calculated diketo, C–H form IV.

tautomers, but this chemical form has not been verified experimentally and since its internal energy is 8.3 kcal/mol higher than keto-enol (II) and 4.5 kcal/mol higher than NH diketo (I), the probability of its existence is very low at room temperature; the good docking performance of C–H diketo (IV) may stimulate further studies to isolate such tautomer form. We conclude that keto-enol (II), depicted in Figure 7, is the most probable tautomer acting at ICAM-1 active site.

3. Experimental section

3.1. Isolation and culture of endothelial cells

Primary endothelial cells were isolated from human umbilical cord as described before.[33] Endothelial cells were cultured in M-199 medium supplemented with 15% fetal calf serum, 2 mM L-glutamine, 100 units/ml penicillin, 100 units/ml streptomycin, 0.25 μg/ml amphotericin and 50 μg/ml-endothelial-cell growth factor

Table 3
Binding energy (kcal/mol) for guests in the pocket of ICAM-1 active site (line 2), and Delta energy for isolated ligands in water (line 3)

(+)EGCG	NH diketo (I)	Keto-enol (II)	Keto-enol (III)	CH diketo (IV)
−77.5	−4.6	−33.2	0.4	−54.7
	4.8	1.0	0.0	9.3

supplemented with heparin (5 U/ml) in gelatin coated tissue culture flasks. For subculture, the cells were dislodged using 0.125% trypsin containing 0.01 M EDTA solution in puck saline and HEPES buffer. Each donor yields about 9–10 million cells after three passages. The cells thus obtained were used as primary cells in our experiments.

3.2. Cell cytotoxicity assay

The cytotoxic effect of tested compounds was determined by using trypan blue exclusion test as described[8] and was further confirmed by colorimetric methyl thiazol tetrazolium (MTT) assay as described.[11] Briefly, endothelial cells were treated with vehicle, DMSO alone (0.25%) or with different concentrations of tested for 24 h. Four hours before the end of incubation, medium was removed and 100 μl of MTT (5 mg/ml in PBS) was added to each well. After 4 h incubation MTT was removed, cells were washed out with PBS, and 50 μl DMSO was added to each well to dissolve water insoluble MTT-formazan crystals. Absorbance was recorded at 570 nm in an ELISA reader (BIO RAD, Model 680, USA).

3.3. Cell-ELISA for measurement of ICAM-1

The cell surface expression of ICAM-1 on endothelial monolayer was quantified using cell-ELISA.[33] Briefly, human umbilical vein endothelial cells were grown to confluency in 96 well flat bottom ELISA plate that was already gelatinized. The cells were incubated with or without β-diketones (**L-1** to **L-6**) or metal diketonates (**C-1** to **C-6**), solubilized in DMSO for desired time, followed by induction with TNF-α. The incubation was continued for 16 h for ICAM-1. The cells were washed with phosphate buffer saline (PBS, pH 7.4) and incubated with 1% gluteraldehyde for 30 min at 4 °C. To inhibit the non-specific binding of antibody, cells were incubated in 3% defatted milk for 3 h at 37 °C, then cells were incubated with anti ICAM-1 monoclonal antibody overnight at 4 °C. Next day cells were washed with PBS and incubated with peroxidase conjugated secondary antibody for 3 h at 37 °C. After washing with PBS, the cells were exposed to the peroxidase substrate (*O*-phenylenediamine dihydrochloride 40 mg/100 ml in citrate buffer pH 4.5). The color development reaction was stopped by 2 N sulfuric acid and absorbance was read at 490 nm by an automated microplate reader (Spectromax 190, Molecular Devices, USA).

3.4. Chemistry

All solvents were dried, degassed, and distilled prior to use. Elemental analyses (C, H, N) were performed with a Fisons Instruments 1108 CHNS-O Elemental analyzer. IR spectra were recorded from 4000 to 100 cm^{-1} with a Perkin–Elmer System 2000 FTIR instrument. ^1H NMR spectra, referenced to $Si(CH_3)_4$, were recorded on a VXR-300 Varian spectrometer (300 MHz for ^1H). Relative intensity of signals is given in square brackets and *J* in hertz.

3.4.1. 4-Furancarbonyl-3-methyl-1-phenylpyrazol-5-one, HQ^{Fur} (L-1)

To a hot dioxane solution of 3-methyl-1-phenylpyrazole-5-one (15 g, 0.088 mol) $Ca(OH)_2$ (12 g, 0.162 mol) was added and the resulting mixture refluxed for 30 min. Then 2-furoylchloride (12.61 g, 0.086 mol) was added dropwise to the suspension and the reaction mixture refluxed for 24 h. The yellow precipitate formed was treated with 350 ml of 2 N HCl and then filtered off and re-crystallized from MeOH. Mp 103–105 °C. Anal. Calcd for $C_{15}H_{12}N_2O_3$: C, 67.16; H, 4.51; N, 10.44. Found: C, 67.19; H, 4.57; N, 10.40. IR (Nujol, cm^{-1}): 2700br ν(O···H), 1625m, 1585s; 1531s ν(C---O, C---C), 690s; 604s; 585s, 509s; 391m; 355s; 282s. ^1H NMR ($CDCl_3$, 300 MHz): δ 2.59 (s, 3H, 3-CH_{3QFur}), 6.62 (t, 1H, C_4H_3O), 7.25 (t, 1H, C_4H_3O), 7.42 (m, 3H, C_6H_5), 7.69 (d, 1H, C_4H_3O), 7.85 (d, 2H, C_6H_5).

3.4.2. 4-Benzoyl-3-methyl-1-phenylpyrazol-5-one, HQ^{Ph} (L-2)

It was synthesized as described for HQ^{Fur} (**L-1**). Anal. Calcd for $C_{17}H_{14}N_2O_2$: C, 73.22; H, 5.27; N, 9.98. Found: C, 73.16; H, 5.16; N, 10.12. Mp 94–96 °C. IR (Nujol, cm^{-1}): 2700br ν(O···H), 1599s,

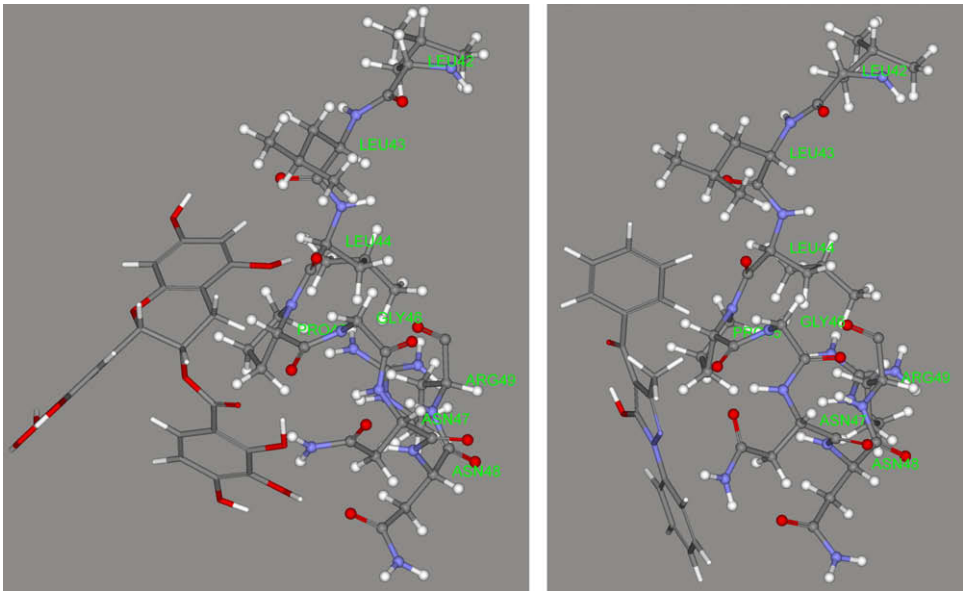

Figure 7. Best fit structures of (+)EGCG (left) and keto-enol (II) tautomer (right) in the active site (Leu42-Arg49) of ICAM-1.

1570s, 1560s, 1554s, 1536sh, s ν(C⋯O, C⋯C), 602m, 533m, 507m, 412w, 400w, 393w, 361w, 328w, 296w, 281w. ^{1}H NMR ($CDCl_3$, 300 MHz): δ 2.11 (s, 3H, 3-CH_{3QPh}), 7.3, 7.5, 7.9 (m, 14H, C_6H_5), 10.5 (s br, 1H, O*H*). ^{13}C NMR ($CDCl_3$): δ 15.8 (s, *C*H_3), 120.8, 126.7, 128.3, 129.1, 131.9, 137.3, 137.6 (s, C_{arom} of C_6H_5), 103.6 (s, *C*3), 148.0 (s, *C*4), 162.5 (s, *C*5), 192.0 (s, *C*O).B.

3.4.3. 4-*t*-Butancarbonyl-3-methyl-1-phenylpyrazol-5-one, HQ^{tBu} (L-3)

It was synthesized as described for compound **L-1**. Mp 88–89 °C. Anal. Calcd for $C_{15}H_{18}N_2O_2$: C, 69.80; H, 7.02; N, 10.81. Found: C, 69.54; H, 7.43; N, 10.65. IR (Nujol, cm^{-1}): 3300br–2800br ν(O···H), 1644s, 1604s, 1555s ν(C⋯O, C⋯C), 610sw, 596m, 504m, 444w, 395w, 333m, 311w. ^{1}H NMR (DMSO-d_6, 300 MHz): δ 1.40 (s, 9H, CH_3*t*Bu) 2.50 (s, 3H, 3-CH_3), 7.3, 7.5, 7.9 (m, 14H, C_6H_5). 13.0 (s br, 1H, O*H*).

3.4.4. 4-(3-Cyclopentylpropanoyl)-3-methyl-1-phenylpyrazol-5-one, HQ^{ETCP} (L-4)

It was synthesized as described for compound **L-1**. Mp 77–78 °C. Anal. Calcd for $C_{18}H_{22}O_2N_2$: C, 72.48; H, 7.38; N, 9.40. Found: C, 71.97; H, 7.23; N, 9.69. IR (Nujol, cm^{-1}): 3000–2800 ν(O···H), 1631, 1594, 1553, 1498 ν(C⋯O, C⋯C), 753, 691, 632, 503. ^{1}H NMR ($CDCl_3$, 295 K, 300 MHz): δ 1.2–2.0 (m, 9H, C_5H_9), 2.51 (s, 3H, 3-CH_3pz), 2.75 (m, 2H, CH_2), 7.27–7.85 (m, 5H, C_6H_5), 12.2 (s br, 1H, O*H*).

3.4.5. 4-*tert*-Butylacetyl-3-methyl-1-phenylpyrazol-5-one, HQ^{nPe} (L-5)

3-Methyl-1-phenylpyrazol-5-one (15.0 g, 0.088 mol) and dry 1,4-dioxane (80 ml) were placed in a flask equipped with a stirrer, separating funnel and a reflux condenser. To this warmed clear solution calcium hydroxide (12.0 g, 0.162 mol) was added. Afterwards, *t*-butylacetyl chloride (11.9 g, 0.086 mol) was dropwise added, in about 10 min. The mixture was refluxed for 4 h and poured into 2 mol dm^{-3} HCl (300 ml) to decompose the calcium complex. The light brown immediately formed precipitate was filtrated and dried under reduced pressure at 50 °C. Re-crystallization was performed by treating the solid with hot methanol and slow cooling of the solution afforded a yellow crystalline powder. Mp 85–87 °C, yield 84%, Anal. Calcd for $C_8H_{10}NO$: C, 70.60; H, 7.40; N, 10.32. Found: C, 70.50; H, 7.50; N, 10.30. IR (Nujol, cm^{-1}): 1642vs, ν(CO); 579s, 509vs, 448w, 419w, 396w, 370m, 356m, 333m, 305w, 270m, 243w and 224w. ^{1}H NMR ($CDCl_3$): δ 2.48 (s, 3 H, CH_{3QnPe}); *2.63s (s, 2H, CH$_2$)*, 1.12 (s, 9H, CH_3); 7.25 (t), 7.46 (t), 7.90 (d), (5H, aromatics), 11.5 (br, 1H, O*H*⋯O). UV/VIS ($CDCl_3$):246 (sh) (11740) and 268 nm (15,380 dm^3 mol^{-1} cm^{-1}).

3.4.6. 4-Benzoyl-3-methyl-1-phenylpyrazol-5-one, HQ^{Ph,Ph,Me} (L-6)

It was synthesized as described for compound **L-1**. Mp 145–147 °C. yield: 72%. MS; *m*/*z*: 278 [M$^+$]. Anal. Calcd for $C_{17}H_{14}N_2O_2$: C, 73.37; H, 5.07; N, 10.07. Found: C, 73.16; H, 5.16; N, 10.12. IR (Nujol, cm^{-1}): ν(OH···O) 2800br; 1622vs (br). ^{1}H NMR ($CDCl_3$): δ 2.18 (s, 3H, CH_3), 3.20 (s br, 1H, N*H*···O), 7.25m, 7.33d, 7.60m, 7.92d (10H, C_6H_5). ^{13}C NMR ($CDCl_3$): δ 26.8 (s, *C*H_3(C=O)), 120.9, 126.8, 128.5, 128.7, 129.1, 129.3, 129.4, 132.9, 137.3 (s, C of C_6H_5), 104.0 (s, *C*3), 151.3 (s, *C*4), 160.5 (s, *C*5), 195.3 (s, *C*O).

3.4.7. bis(4-*t*-Butylacetyl-3-methyl-1-phenylpyrazol-5onato)bis(ethanol)calcium(II), [Ca(Q^{nPe})$_2$(EtOH)$_2$] (C-1)

An ethanolic solution (30 ml) of HQ^{nPe} (2 mmol) and KOH (2 mmol) were added to an aqueous solution (10 ml) of calcium dichloride (1 mmol). In a few minutes a white precipitate formed. After 1 h stirring the precipitate was filtered, washed with water (10 ml) and dried under reduced pressure at 50 °C. Re-crystallization from hot ethanol gave colorless crystals on cooling. Mp 329–331 °C, yield 84%. Anal. Calcd for $C_{36}H_{50}CaN_4O_6$: C, 64.07; H, 7.47; N, 8.30. Found: C, 63.82; H, 7.55; N, 8.46. IR (Nujol, cm^{-1}): 3500–2400br, ν(OH···N) 1644s, δ(OH); 1591vs, *n*(C]] O); 440vs, 409m, ν_{sym} (Ca–O); 377m, 253vs (br), 233m, ν_{asym}(Ca–O). ^{1}H NMR ($CDCl_3$): *d* 2.39 (s, 6H, CH_3), 2.43 (s, 4H, CH_2), 0.90 (s, 18H, CH_3); 6.67 (d) 7.05 (t), 7.24 (t), (10H, aromatics); 1.71 (t, 6 H, CH_{3EtOH}), 3.64 (q, 4 H, CH_{2EtOH}).

3.4.8. bis(4-*tert*-Butylacetyl-3-methyl-1-phenylpyrazol-5-onato)bis(aquo)zinc(II), [Zn(Q^{nPe})$_2$(H$_2$O)$_2$], (C-2)

It was synthesized reacting $Zn(O_2CCH_3)_2{\cdot}2H_2O$ (0.219 g, 1.0 mmol) with HQ^{nPe} (0.545 g, 2.0 mmol) in 30 ml of MeOH at rt. From the solution a pale yellow solid slowly precipitated. The suspension was stirred 4 h and filtered. The precipitate was washed with Et_2O and dried to constant weight under reduced pressure. Recrystallized from $CHCl_3$/*n*-hexane. Mp 185–189 °C, yield 79%. Anal. Calcd for $C_{32}H_{40}N_4O_5Zn$: C, 61.39; H, 6.44; N, 8.95. Found: C, 61.50; H, 6.60; N, 9.21. Λ_m (in acetone): 5.0 Ω^{-1} cm^2 mol^{-1}. IR (Nujol, cm^{-1}): 3000–3200br (O–H···N), 1608s (C=O), 466sbr, 350m (Zn–O). ^{1}H NMR ($CDCl_3$): δ, 1.10 (s) (18 H, (CH_3)$_3$CCH$_2$C(=O)), 2.15 (br) (2H, H_2O), 2.50 (s) (6H, 3-CH_3), 2.65 (s) (18H, $(CH_3)_3CCH_2C(=O)$), 7.30 (m), 7.92 (m) (10H, C_6H_5).

3.4.9. (4-Benzoyl-3-methyl-1-phenylpyrazol-5-onato)sodium, [NaQ^{Ph}], (C-3)

It was synthesized reacting Na(OMe) (0.108 g, 2.0 mmol) with HQ^{Ph} (0.545 g, 2.0 mmol) in 30 ml of MeOH at rt. The clear solution was stirred overnight, then evaporated and the residue washed with Et_2O and dried to constant weight under reduced pressure. Mp 185–189 °C, yield 90%. Anal. Calcd for $C_{17}H_{13}N_2NaO_2$: C, 68.00; H, 4.36; N, 9.33. Found: C, 67.45; H, 4.60; N, 9.12. IR (Nujol, cm^{-1}): 1620sh, 1605s, 1592s ν(C⋯O, C⋯C), 602m, 540m, 504m, 404w, 329w. ^{1}H NMR ($CDCl_3$, 300 MHz): δ 1.85 (s, 3H, 3-CH_{3QPh}), 7.2, 7.4, 7.7 (m, 14H, C_6H_5).

3.4.10. Sodium(benzoylacetonato), [Na(bzac)]·H$_2$O, (C-4)

It was synthesized reacting Na(OMe) (0.108 g, 2.0 mmol) with benzoylacetone, bzacH (0.160 g, 1.0 mmol) in 30 ml of MeOH at rt. The clear solution was stirred overnight, then evaporated and the residue washed with Et_2O and dried to constant weight under reduced pressure. Mp 100–104 °C, yield 90%. Anal. Calcd for $C_{10}H_{10}O_3Na$: C, 59.41; H, 5.48. Found: C, 59.23; H, 5.24. IR (Nujol, cm^{-1}): 1605s, 1554s, 1503s, ν(C⋯O, C⋯C), 588m, 547m, 497w, 428w, 398w, 301w. ^{1}H NMR (CD_3OD, 300 MHz): δ 2.28 (s, 3H, CH_3), 7.4m (4H, C_6H_5 + CH_{bzac}) 7.8 (2H, C_6H_{5bzac}).

3.4.11. Sodium(benzoyltrifluoroacetonato), [Na(bzfc)], (C-5)

It was synthesized reacting Na(OMe) (0.108 g, 2.0 mmol) with benzoyltrifluoroacetone, bzfcH (0.216 g, 1.0 mmol) in 30 ml of MeOH at rt. The clear solution was stirred overnight, then evaporated and the residue washed with Et_2O and dried to constant weight under reduced pressure. Mp 256–261 °C, yield 80%. Anal. Calcd for $C_{10}H_6F_3O_2Na$: C, 50.44; H, 2.54. Found: C, 50.23; H, 2.76. IR (Nujol, cm^{-1}): 1605s, 1554s, 1503s, ν(C⋯O, C⋯C), 633s, 575s, 513w, 492m, 441w, 367s br, 305w. ^{1}H NMR (CD_3OD, 300 MHz): 5.99 (s, 1H, CH_{bzfc}) 7.36m, 7.79m (5H, C_6H_{5bzfc}).

3.4.12. bis(4-Pivaloyl-3-methyl-1-phenylpyrazol-5-onato)bis(aqua)zinc(II), [Zn(Q^{tBu})$_2$(H$_2$O)$_2$], (C-6)

It was synthesized reacting $Zn(O_2CCH_3)_2{\cdot}2H_2O$ (0.219 g, 1.0 mmol) with HQ^{tBu} (0.530 g, 2.0 mmol) in 30 ml of MeOH at rt. From the solution a pale yellow solid slowly precipitated. After stirring 4 h the suspension was filtered. The precipitate was washed with Et_2O and dried to constant weight under reduced

pressure. Re-crystallised from $CHCl_3$/*n*-hexane. Mp 176–180 °C, yield 79%. Anal. Calcd for $C_{30}H_{38}N_4O_6Zn$: C, 58.49; H, 6.22; N, 9.09. Found: C, 58.55; H, 6.30; N, 9.13. IR (Nujol, cm^{-1}): 3640s (O–H···N), 1608s, 1593s, 1583s, 1502s (C=O), 519w, 503m, 489m, 420s, 411w, 386w, 363w, 324w, 299w (Zn–O). ^1H NMR ($CDCl_3$): δ, 1.25 (s) (18 H, $(CH_3)_3CC(=O)$), 2.60 (br, 6 H, 3-CH_3), 7.20, 7.70 (m, 10H, C_6H_5).

3.5. Theoretical calculations

The structural features of four HQ^{Ph} tautomers (Scheme 3) were analyzed with density functional theory using the Accelrys[34] package Materials Studio 4.1, code DMOL3.[35–37] The effect of water solvent was included using a COSMO algorithm.[38] We used the general gradient approximation (GGA) and the Becke exchange (BP) functional.[39] The highest available DMOL3 level of theory was used including a double numeric basis set[35] with polarization functions (DNP)[39,40] for an all electron calculation. Initial coordinates were those obtained from crystal structures, N–H diketo[27] and keto-enol[28] for tautomers I and II, respectively. Forms III and IV were calculated after modification of calculated structures I and II using DMOL3 subroutines. Converged energies are shown in Table 2. Docking studies for all 4 tautomers and the reference compound (+)EGCG were performed with the CDOCKER package in Discovery Studio 2.1 from Accelrys,[41] the active site radius was of 12 Å in the conformer simulation for each ligand.

3.6. Statistical analysis

Results are given as mean ± SD. Independent two-tailed Student's *t*-test was performed. Differences were considered statistically significant for $P < 0.05$. All statistical analyses were performed using software Microcal Origin (ver 3.0; Microcal Software Inc., Northampton, MA).

4. Conclusion

In this study the ICAM-1 inhibitory activity of curcumin models lacking aromatic peripheral hydroxyl and methoxy groups (β-diketones), and their metal derivatives are investigated experimentally and theoretically. β-Diketones are systematically more active at lower concentrations than their metal complexes; the highest inhibition for both groups is 75%. Among the ligands, the best inhibitor is 4-benzoyl-3-methyl-1-phenyl-pyrazol-5-one (HQ^{Ph}). For this reason, the four tautomeric forms of HQ^{Ph} were investigated using density functional theory. In addition, docking of all HQ^{Ph} tautomers on ICAM-1 protein was performed and suggested that keto-enol (II), depicted in Figures 4 and 7, was favored to act in biological environment.

Acknowledgements

This work is supported by Council of Scientific and Industrial Research (CSIR, India), Task Force Project NWP0033, and by CSIR-CNR (Indio-Italian) bilateral agreement. S.K. and S.B. thank CSIR for their Fellowships. F.C. thanks Vassar College for facilities provided in using DMOL3 program.

References and notes

1. Osborn, L. *Cell* **1990**, *62*, 3.
2. Springer, T. A. *Cell* **1994**, *76*, 301.
3. Collins, T.; Read, M. A.; Neish, A. S.; Whitley, M. Z.; Thanos, D.; Maniatis, T. *FASEB J.* **1995**, *9*, 899.
4. Gorski, A. *Immunol. Today* **1994**, *15*, 251.
5. Mantovani, A.; Bussolino, F.; Introna, M. *Immunol. Today* **1997**, *18*, 231.
6. Butcher, C. E. *Cell* **1991**, *67*, 1033.
7. Weiser, M. R.; Gibbs, S. A. L.; Hechtman, H. B. In *Adhesion Molecules in Health and Disease*; Paul, L. C., Issekutz, T. B., Eds.; Marcel Dekker: New York, 1997; p 55.
8. Madan, B.; Batra, S.; Ghosh, B. *Mol. Pharmacol.* **2000**, *58*, 526.
9. Kumar, S.; Singhal, V.; Roshan, R.; Rambotkar, G. W.; Ghosh, B. E. *J. Pharmacol.* **2007**, *73*, 1602.
10. Kumar, S.; Singh, B. K.; Kalra, N.; Kumar, V.; Kumar, A.; Raj, H. G.; Prasad, A. K.; Parmar, V. S.; Ghosh, B. *Bioorg. Med. Chem.* **2005**, *13*, 1605.
11. Kumar, S.; Arya, P.; Mukherjee, C.; Singh, B. K.; Singh, N.; Parmar, V. S.; Prasad, A. K.; Ghosh, B. *Biochemistry* **2005**, *44*, 15944.
12. Madan, B.; Ghosh, B. *Shock* **2003**, *19*, 91.
13. Singh, N.; Kumar, S.; Singh, P.; Raj, H. G.; Prasad, A. K.; Parmar, V. S.; Ghosh, B. *Phytomedicine* **2008**, *4*, 284.
14. Shibata, S. *Yakugaku Zasshi* **2000**, *120*, 849.
15. Ram, A.; Mahabalirajan, U.; Das, M.; Bhattacharya, I.; Dinda, A. K.; Gangal, S. V.; Ghosh, B. *Int. Immunopharmacol.* **2006**, *9*, 1468.
16. Kumar, S.; Sharma, A.; Madan, B.; Singhal, V.; Ghosh, B. *Biochem. Pharmacol.* **2007**, *73*, 1602.
17. Kim, Y. S.; Ahn, Y.; Hong, M. H.; Joo, S. Y.; Kim, K. H.; Sohn, I. S.; Park, H. W.; Hong, Y. J.; Kim, J. H.; Kim, W.; Jeong, M. H.; Cho, J. G.; Park, J. C.; Kang, J. C. *J. Cardiovasc. Pharmacol.* **2007**, *50*, 41.
18. Lin, C.-C.; Lee, C.-W.; Chu, T.-H.; Cheng, C.-Y.; Luo, S.-F.; Hsiao, L.-D.; Yang, C.-M. *J. Cell. Physiol.* **2007**, *211*, 771.
19. Kunnumakkara, A. B.; Guha, S.; Krishnan, S.; Diagaradjane, P.; Gelovani, J.; Aggarwal, B. B. *Cancer Res.* **2007**, *67*, 3853.
20. Mitra, A.; Chakrabarti, J.; Banerji, A.; Chatterjee, A.; Das, B. R. *J. Environ. Pathol. Toxicol. Oncol.* **2006**, *25*, 679.
21. Punithavathi, D.; Babu, M.; Arumugam, V.; Venkatesan, N. *Lett. Drug Des. Discovery* **2006**, *3*, 714.
22. Caruso, F.; Rossi, M.; Tanski, J.; Sartori, R.; Sariego, R.; Moya, S.; Diez, S.; Navarrete, E.; Cingolani, A.; Marchetti, F.; Pettinari, C. *J. Med. Chem.* **2000**, *43*, 3665.
23. Pettinari, C.; Caruso, F.; Zaffaroni, N.; Villa, R.; Marchetti, F.; Pettinari, R.; Phillips, C.; Tanski, J.; Rossi, M. J. *Inorg. Biochem.* **2006**, *100*, 58.
24. Bischoff, H.; Berger, M. R.; Keppler, B. K.; Schmaehl, D. J. *Cancer Res. Clin. Oncol.* **1987**, *113*, 446.
25. Keppler, B. *K.; Friesen, C.; Vongerichten, H.; Vogel, E. In Metal Complexes in Cancer Chemotherapy; Keppler, B. K*; Ed.; VCH: Weinheim, Germany, 1993. pp 297–323.
26. Kumar, A.; Dhawan, S.; Hardegen, N. J.; Aggarwal, B. B. *Biochem. Pharmacol.* **1998**, *55*, 775.
27. O'Connell, M. J.; Ramsay, C. G.; Steel, P. J. *Aust. J. Chem.* **1985**, *38*, 401.
28. Akama, Y.; Shiro, M.; Ueda, T.; Kajitani, M. *Acta Crystallogr., Sect. C* **1995**, *51*, 1310.
29. Pettinari, C.; Marchetti, F.; Cingolani, A.; Lorenzotti, A.; Mundorff, E.; Rossi, M.; Caruso, F. *Inorg. Chim. Acta* **1997**, *262*, 33.
30. Tse, M. T.; Chakrabarti, K.; Gray, C.; Chitnis, C. E.; Craig, A. *Mol. Microbiol.* **2004**, *51*, 1039.
31. Dormeyer, M.; Adams, Y.; Kramer, B.; Chakravorty, S.; Tse, M. T.; Pegoraro, S.; Whittaker, L.; Lanzer, M.; Craig, A. *Antimicrob. Agents Chemother.* **2006**, *50*, 724.
32. Bella, J.; Kolatkar, P. R.; Marlor, C. W.; Greve, J. M.; Rossmann, M. G. *Proc. Natl. Acad. Sci. U.S.A.* **1998**, *95*, 4140.
33. Kumar, S.; Singh, B. K.; Pandey, A. K.; Kumar, A.; Sharma, S. K.; Raj, H. G.; Prasad, A. K.; Van der Eychen, E.; Parmar, V. S.; Ghosh, B. *Bioorg. Med. Chem.* **2007**, *15*, 1952.
34. Accelrys Inc. Materials Studio Release 4.1. 10188 Telesis Court, Suite 100, San Diego, CA 92121, USA.
35. Delley, B. *J. Chem. Phys.* **1990**, *92*, 508.
36. Delley, B. *J. Chem. Phys.* **2000**, *113*, 7756.
37. Delley, B. *J. Phys. Chem.* **1996**, *100*, 6107.
38. Klamt, A.; Schrmann, G. *J. Chem. Soc., Perkin Trans.* **1993**, *2*, 799.
39. Becke, A. D. *Phys. Rev.* **1988**, *A38*, 3098.
40. Perdew, J. P.; Chevary, J. A.; Vosko, S. H.; Jackson, K. A.; Pederson, M. R.; Singh, D. J.; Fiolhais, C. *Phys. Rev. B: Condens. Matter Mater. Phys.* **1992**, *46*, 6671.
41. Wu, G.; Robertson, D. H.; Brooks, C. L., III; Vieth, M. *J. Comput. Chem.* **2003**, *24*, 1549.